Supplementary information for

Performance study of Zn-Co-Ni/AC catalyst in acetylene acetylation

Zhuang Xu[a], Peijie He[a], Yuhao Chen[a], Mingyuan Zhu[a,b], Xugen Wang[a,b*]and

Bin Dai[a,b*]

a School of Chemistry and Chemical Engineering of Shihezi University, Shihezi, Xinjiang 832000, PR China.

b Key Laboratory for Green Processing of Chemical Engineering of Xinjiang Bingtuan, Shihezi, Xinjiang
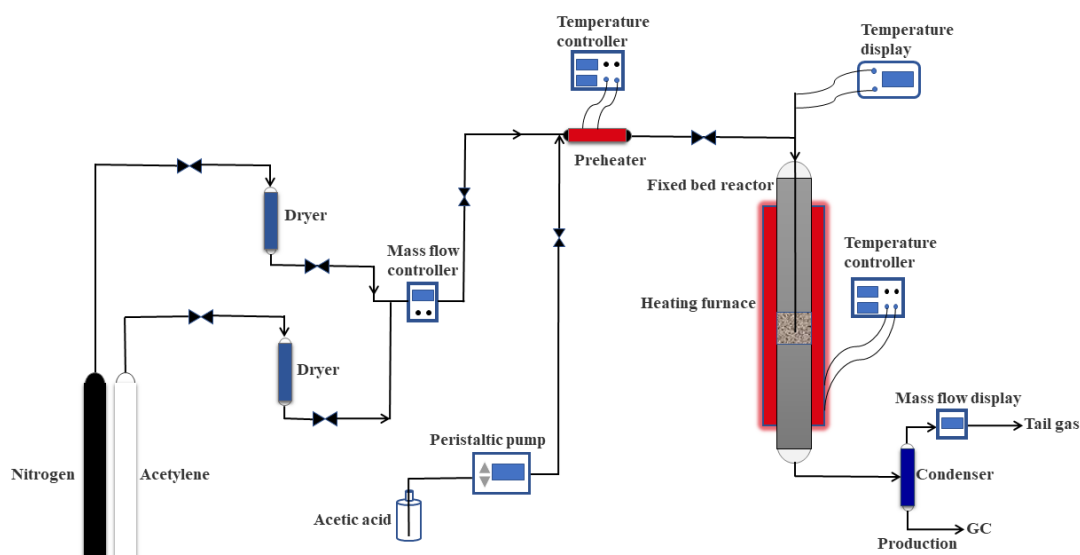
832000, PR China.

Figure S1. Flow Chart-Experimental setup.

Table S1. Calculation of carbon balance.

Catalyst	C_{Feed} [a] in the Reactor (g)	C_{Outlet} [b] in the Gas Phase (g)	C_{Outlet} [c] in the Liquid Phase (g)	C_{Outlet} [d] in the Solid Phase (g)	Carbon Balance (%)
Zn-Co-Ni/AC	348.22	242.33	88.14	0.164	94.9
Zn(OAc)₂/AC	348.22	269.54	46.34	0.421	90.8

[a]The mass of carbon fed into the reactor. [b]The mass of carbon outlet in the gas phase. [c]The mass of carbon outlet in the liquid phase. [d]The mass of carbon outlet in the solid phase.

The calculation of carbon balance after catalytic test as shown in Table S1. The mass of C entering the reactor was calculated as the total amount of reactants entering the reactor during the reaction time. The mass of C at the reactor outlet were calculated as the sum of the mass of acetylene in the tail gas and the mass of carbon deposition obtained through the TG. All the products in the liquid phase were obtained by chromatographic analysis. The conclusion from Table S1 was that the carbon balance values were higher than 90% for the Zn-Co-Ni/AC and Zn(OAc)₂/AC catalysts, addition of co-catalyst improved the carbon balance caused by the reduction of carbon deposition.
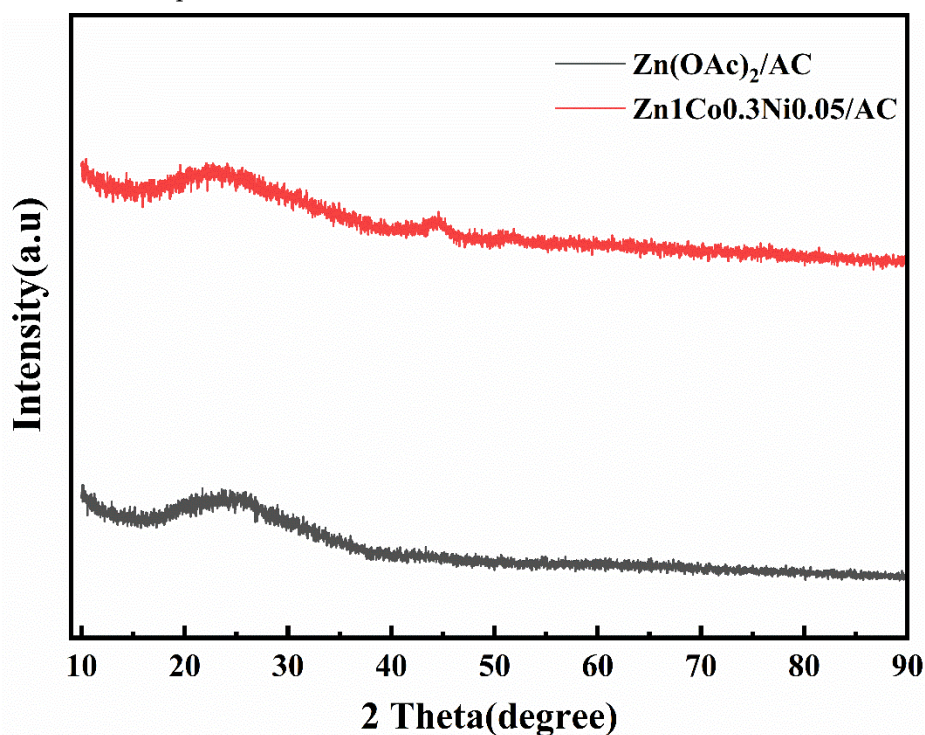

Figure S2. X-ray diffraction patterns for Zn(OAc)₂/AC and Zn1Co0.3Ni0.05/AC catalysts.

As shown in Fig.S2, the Zn(OAc)₂/AC and Zn1Co0.3Ni0.05/AC samples show two diffraction peaks at two thetas of 25° and 42.5°, attribute to the (002) and (100) reflection of carbon. In our previous work[1-4], we found that the interaction force between the active component and the carrier was weak, so the crystal shape of active component on activated carbon carriers was found to be amorphous.
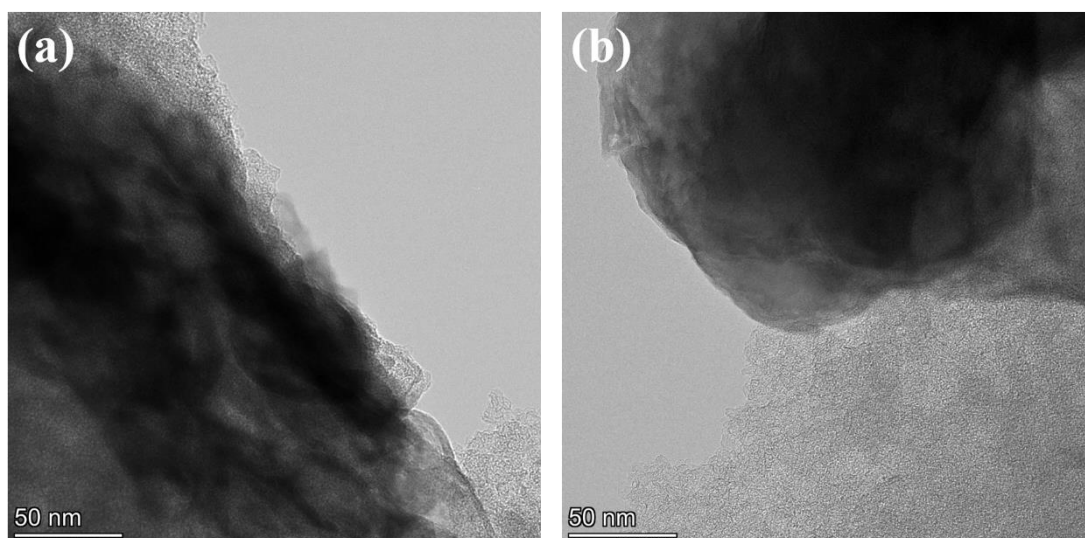
Figure S3. TEM image for Zn(OAc)$_2$/AC(a) and Zn1Co0.3Ni0.05/AC(b) catalysts.

The combination of TEM and XRD shows that the active component is amorphously dispersed on the carrier. From the EDS data (Table S2), it can be concluded that nickel and cobalt elements are present on the Zn1Co0.3Ni0.05/AC catalyst, but not on the Zn (OAc)$_2$/AC catalyst. This also demonstrates the successful preparation of Zn1Co0.3Ni0.05/AC catalyst.

Table S2. Element content of Zn(OAc)$_2$/AC and Zn1Co0.3Ni0.05/AC catalysts.

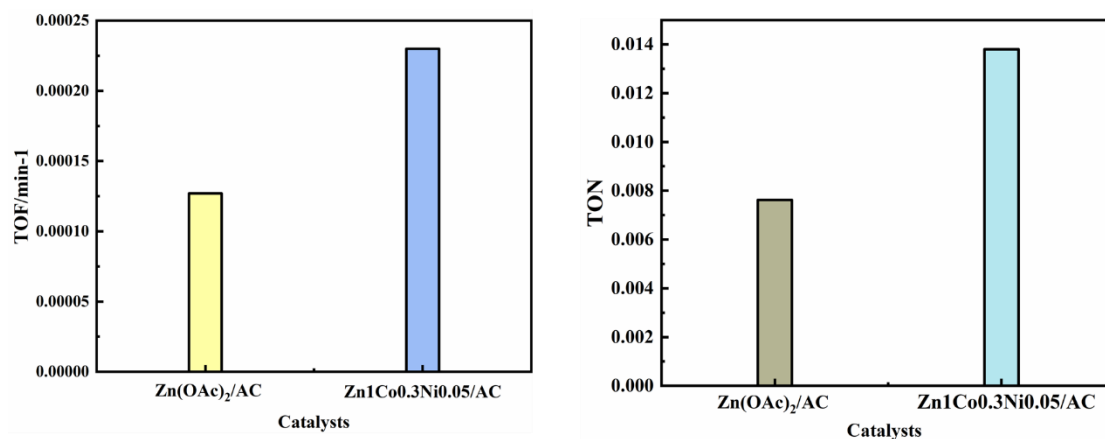| Sample	Element content (%) (EDS)				
	C	O	Zn	Co	Ni
Zn(OAc)$_2$/AC	60.13	18.85	21.02	-	-
Zn1Co0.3Ni0.05/AC	43.76	34.91	17.56	3.66	0.11

Figure S4. TOF and TON of catalysts.

The turnover frequency (TOF) of the $Zn(OAc)_2$/AC and Zn1Co0.3Ni0.05/AC catalysts was calculated to evaluate the catalytic performance more directly[5], as illustrated in Fig.S4. The TOF of $Zn(OAc)_2$/AC (1.27×10^{-4} min^{-1}) was 81.1% of that of Zn1Co0.3Ni0.05/AC (2.30×10^{-4} min^{-1}). The turnover number (TON) of $Zn(OAc)_2$/AC and Zn1Co0.3Ni0.05/AC were 7.62×10^{-3} and 1.37×10^{-2}. It can be concluded that the acetylene acetoxylation rate on Zn1Co0.3Ni0.05/AC exceeded that on $Zn(OAc)_2$/AC due to an increase in the dispersity of the Zn particles.

We used a software called ImageJ[6-9]. Detailed description of the particle size distribution (PSD) measurement process. (Figures S5-S12)
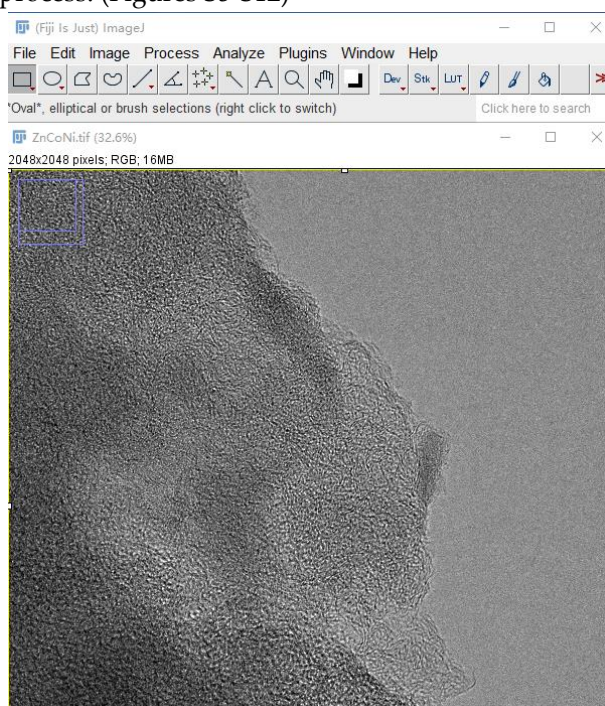

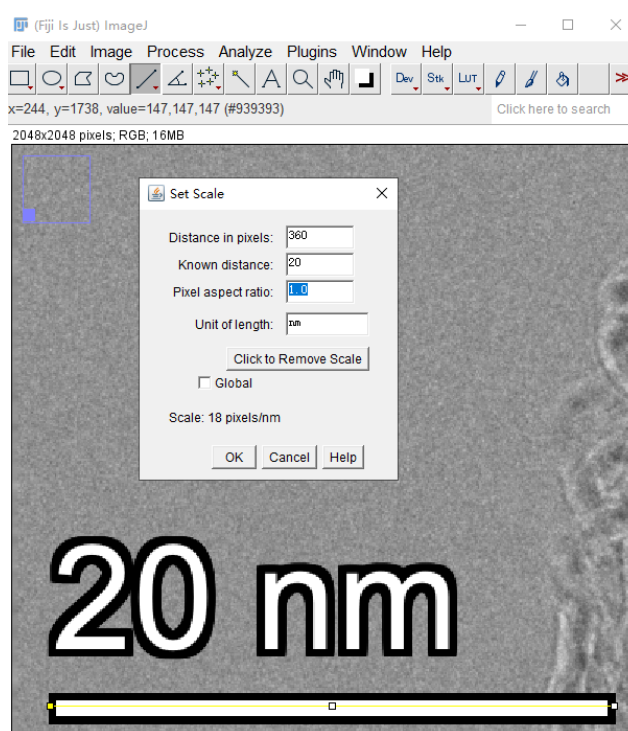**Figure S5.** Step 1: Import the TEM images into the ImageJ software.

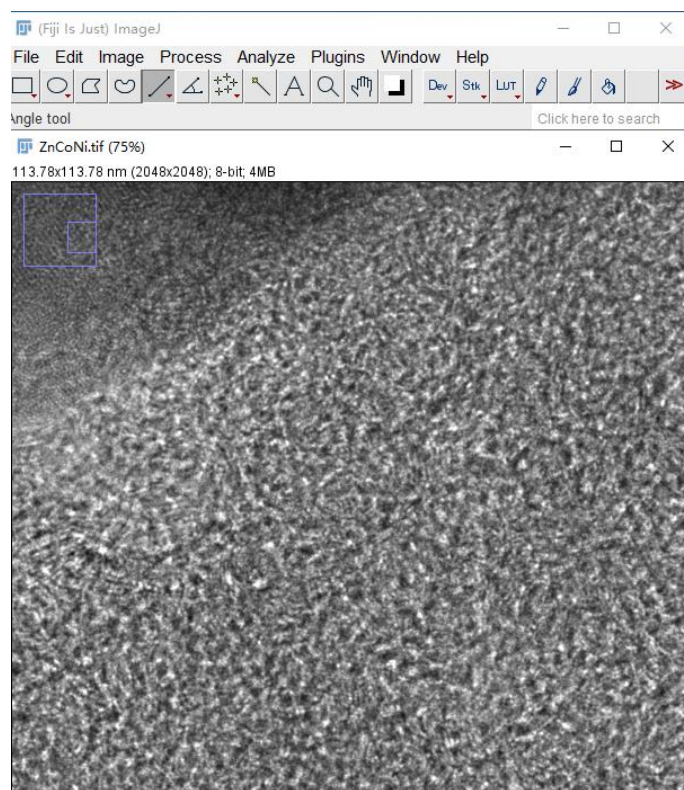

Figure S6. Step 2: Setting the scale.

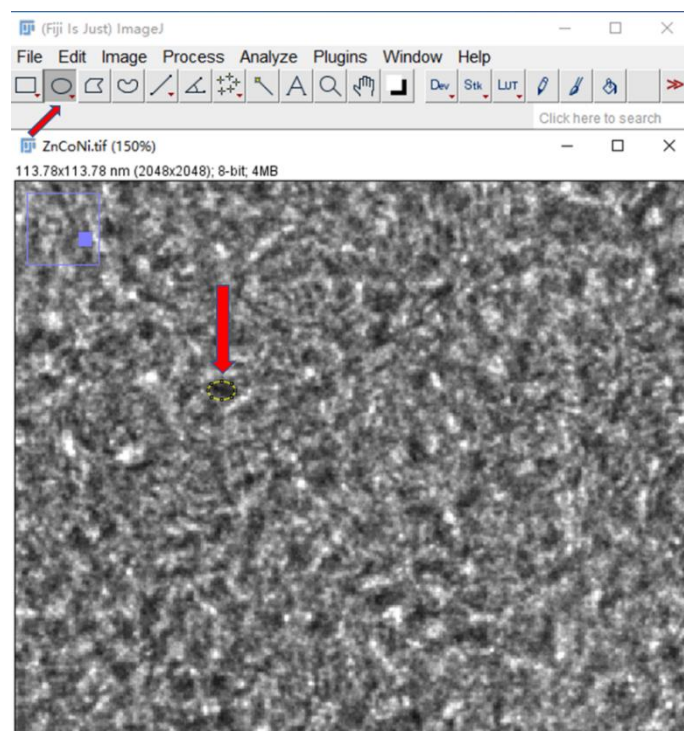**Figure S7.** Step 3: Enlargement of TEM image.

Figure S8. Step 4: Finding the nanoparticle and using the ellipse tool to marking them.
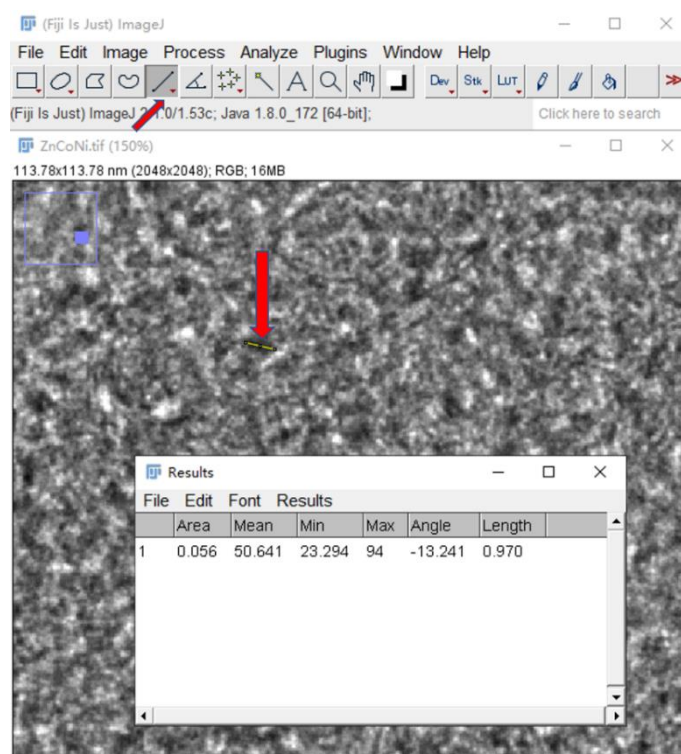
Figure S9. Step 5: Take measurements using the linear tool. Repeat steps 3 and 4 to measure at least 200 nanoparticles.
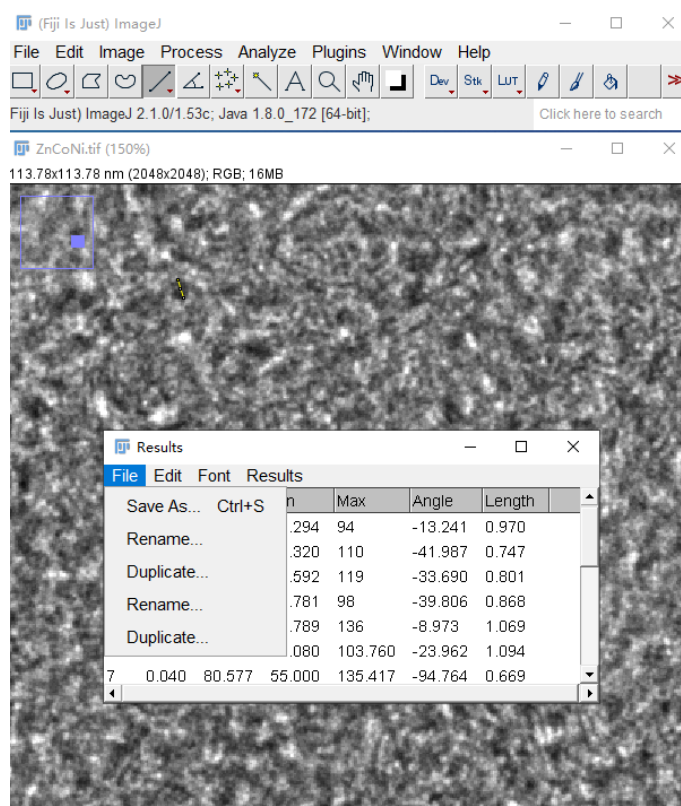

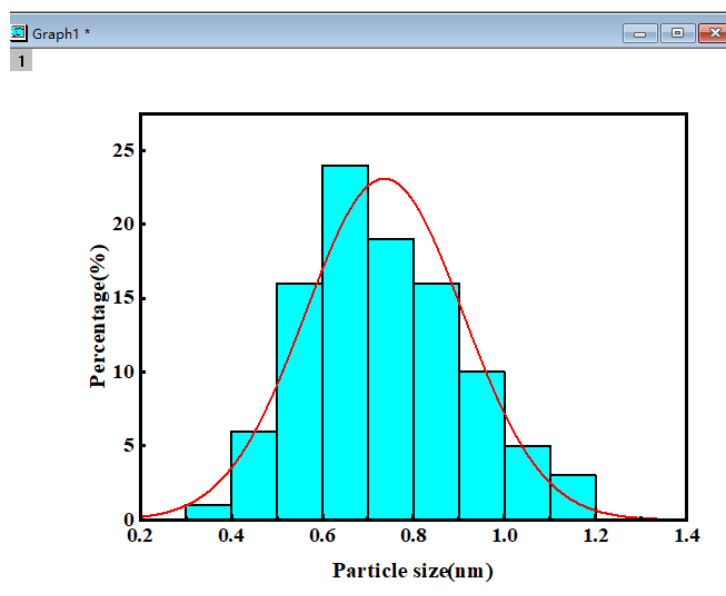**Figure S10.** Step 6: Exporting measurement data.

Figure S11. Step 7: Using the data exported in step 6 to make a graph in origin software.
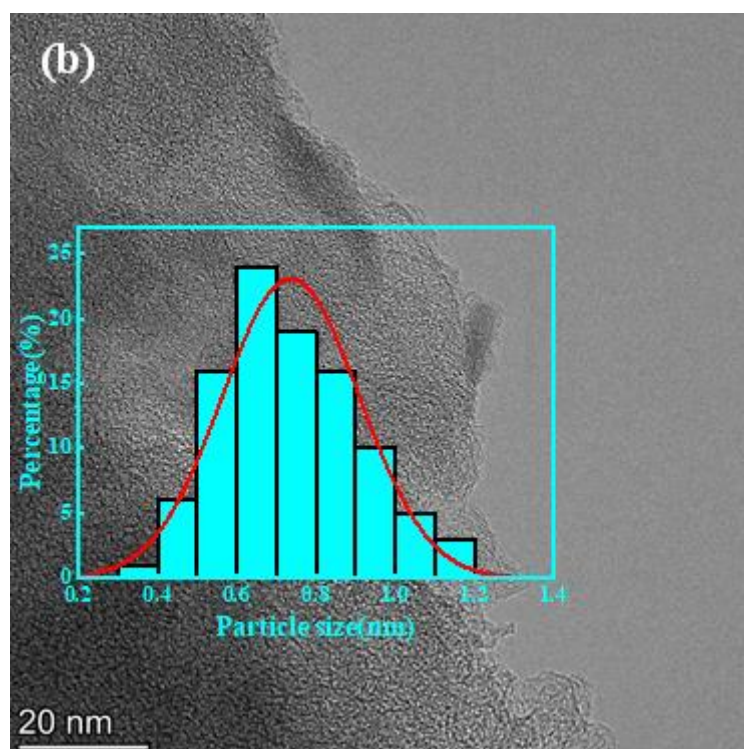

Figure S12. Step 8: Combine the plot made by origin software with the TEM image imported in the first step.

TEM images of fresh $Zn(OAc)_2$/AC and $Zn1Co0.3Ni0.05$/AC catalysts are shown in Figure S13. The average particle sizes of the fresh $Zn(OAc)_2$/AC and $Zn1Co0.3Ni0.05$/AC catalysts are about 1.08 ± 0.34 nm and 0.73 ± 0.17 nm, respectively. This indicates that the addition of Co and Ni can disperse the Zn particles to some extent and resulting in a more uniform dispersion of the active components.
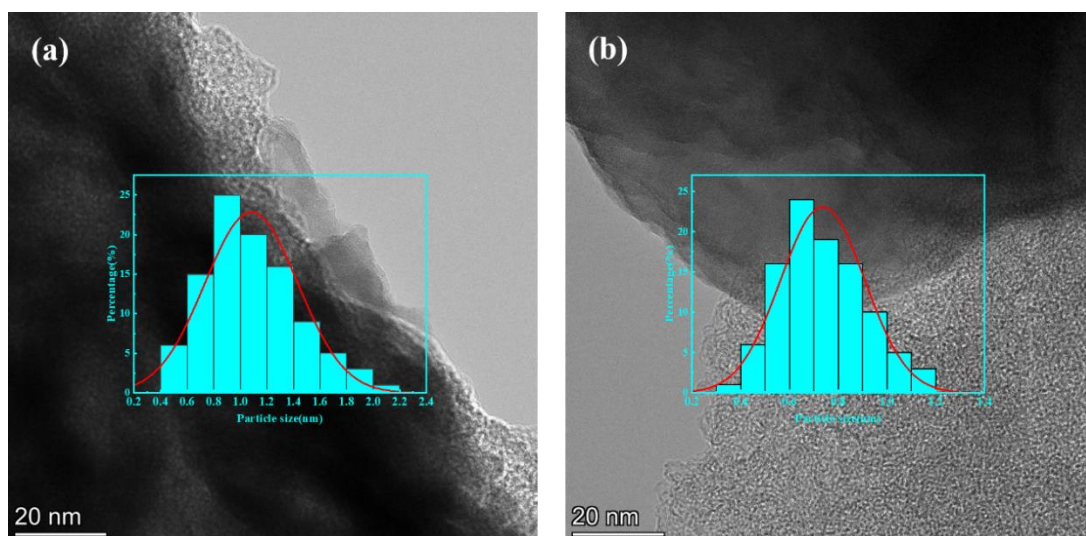
Figure S13. TEM images of catalysts: (a) $Zn(OAc)_2$/AC, (b) Zn1Co0.3Ni0.05/AC.

During the reaction, the reaction products were analyzed in this work using a gas chromatograph, and the results are shown in the Figure S14 (attached below). We also put this part of the content into ESI. The main products in the reaction for the preparation of vinyl acetate from calcium carbide acetylene are VAc (>96% selectivity) and unreacted acetic acid, in addition to small amounts of by-products acetaldehyde.
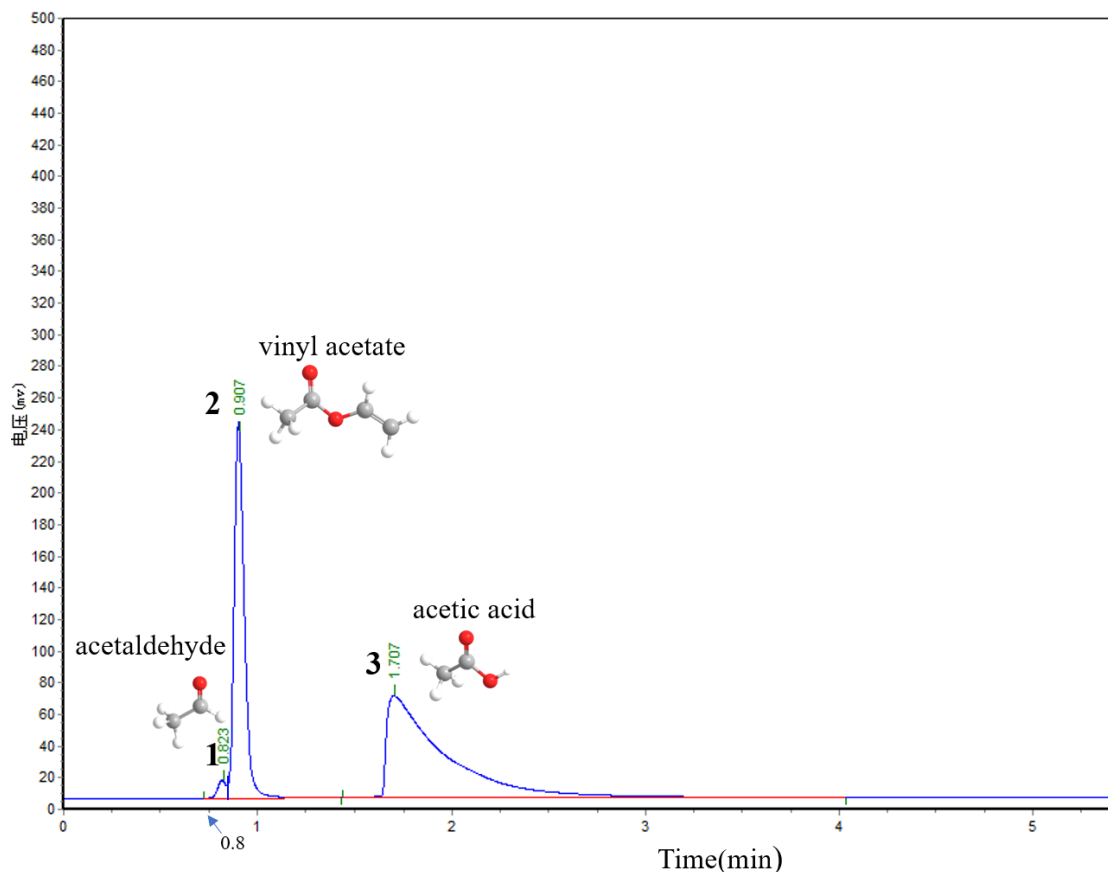

Figure S14. Gas chromatogram spectrum of the products. 1.acetaldehyde 2. vinyl acetate 3. acetic acid.

By reviewing the literature[10], the substances contained in the products were known, using the internal standard method, the main product was identified as vinyl acetate and the by-product as acetaldehyde. Because the raw material acetic acid contains water, the following chemical reactions ($C_2H_2+H_2O \rightarrow CH_3CHO$) have occurred.

The results are shown in the Figure S15-S17 (attached below). The conversion of acetic acid and the selectivity to VAc were calculated as follows:

$$\text{Conversion} = \frac{n_0 - n_1}{n_0} \times 100\%$$

$$\text{Selectivity} = \frac{n_p}{n_0 - n_1} \times 100$$

Wherein, n_0 represents the amount of acetic acid for feedstock before reaction; n_1 denotes amount of acetic acid for residue after reaction and n_p is amount of acetic acid for forming VAc.
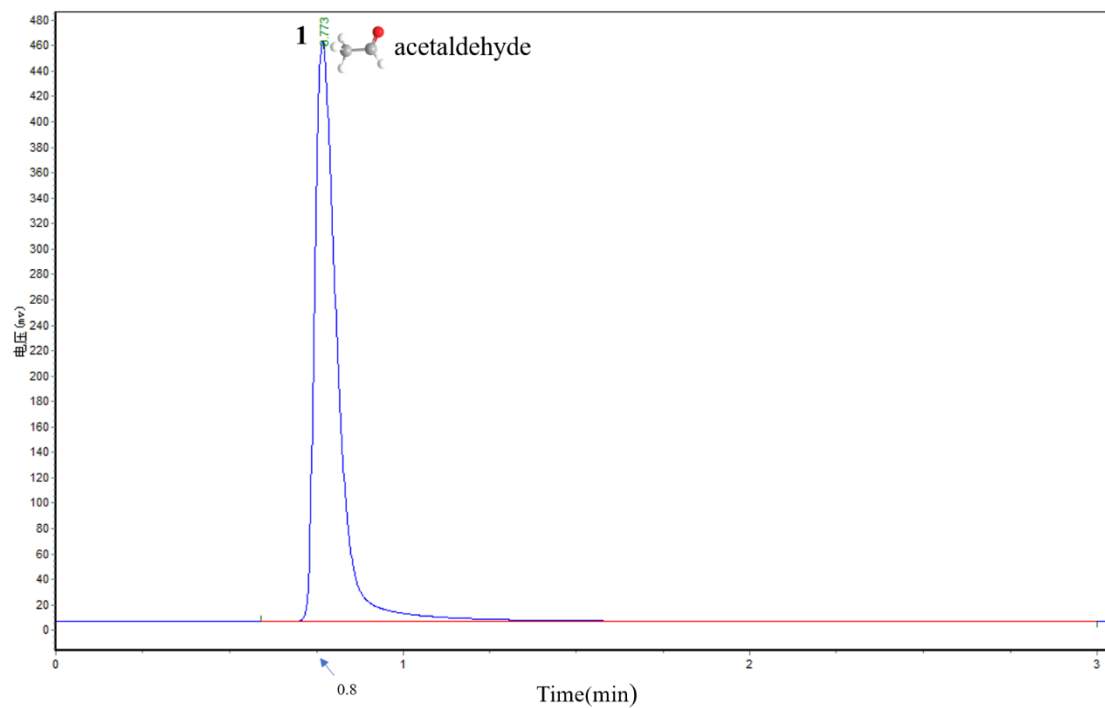
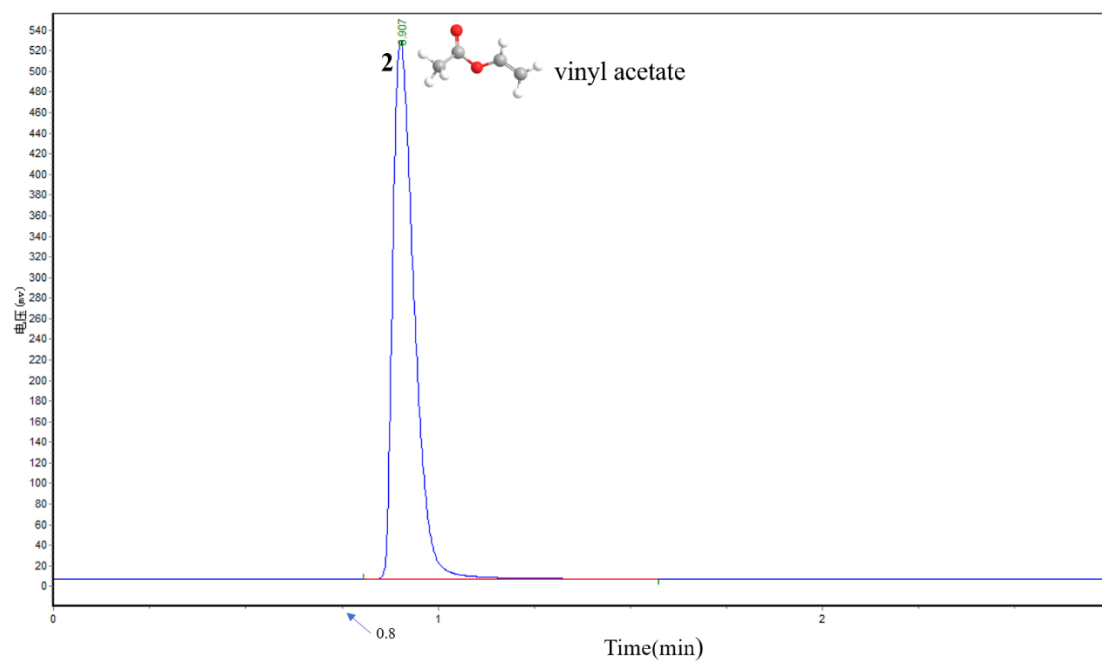**Figure S15.** Gas chromatogram spectrum of the products (acetaldehyde).

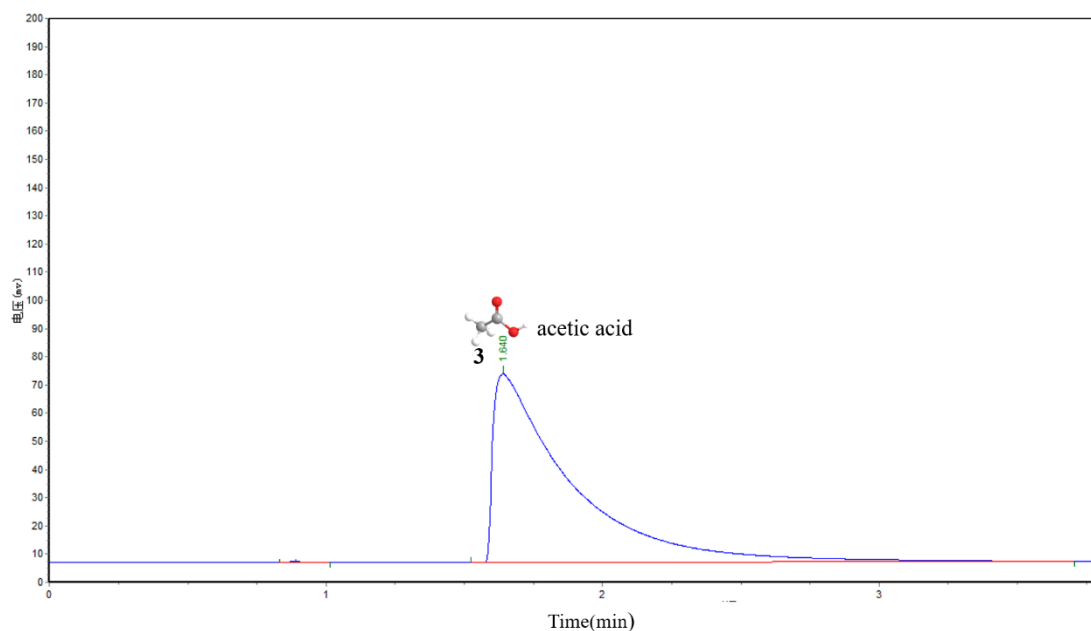**Figure S16.** Gas chromatogram spectrum of the products (vinyl acetate).

Figure S17. Gas chromatogram spectrum of the products (acetic acid).

References：

1. Wu, X.Y.; He, P.J.; Wang, X.G.; Dai, B. Zinc acetate supported on N-doped activated carbon as catalysts for acetylene acetoxylation. *Chemical Engineering Journal* **2017**, *309*, 172-177, doi:10.1016/j.cej.2016.09.090.

2. He, P.J.; Huang, L.H.; Wu, X.Y.; Xu, Z.; Zhu, M.Y.; Wang, X.G.; Dai, B. A Novel High-Activity Zn-Co Catalyst for Acetylene Acetoxylation. *Catalysts* **2018**, *8*, doi:Artn 239 10.3390/Catal8060239.

3. Zhu, F.; Li, J.; Zhu, M.; Kang, L. Effect of Oxygen-Containing Group on the Catalytic Performance of Zn/C Catalyst for Acetylene Acetoxylation. *Nanomaterials* **2021**, *11*, 1174.

4. He, P.J.; Wu, X.Y.; Huang, L.H.; Zhu, M.Y.; Wang, X.G.; Dai, B. Acetoxylation of acetylene to vinyl acetate monomer over bimetallic Zn-Ni/AC catalysts. *Catalysis Communications* **2018**, *112*, 5-9, doi:10.1016/j.catcom.2018.02.022.

5. Zhu, M.; Wang, Q.; Chen, K.; Wang, Y.; Huang, C.; Dai, H.; Yu, F.; Kang, L.; Dai, B. Development of a Heterogeneous Non-Mercury Catalyst for Acetylene Hydrochlorination. *ACS Catalysis* **2015**, 5306-5316.

6. Rasband, W.S. ImageJ - Image Processing and Analysis in Java. *astrophysics source code library* **2012**.

7. Broeke, J.; Perez, J.; Pascau, J. *Image Processing with ImageJ - 2nd Edition*; Image Processing with ImageJ - 2nd Edition: 2015.

8. Abramoff, M.; Magelhaes, P.J.; Ram, S.J. Image Processing with ImageJ. *Biophotonics International* **2003**, *11*, 36-42.

9. Paszek, M.; Dufort, C.; Ru Ba Shkin, M.; Davidson, M.; Thorn, K.; Liphardt, J.; Weaver, V.; Schneider, C.; Ras Ba Nd, W.; Eliceiri, K. 671 nih image to imageJ: 25 years of image analysis. **2012**.

10. Zhang, M.; Fu, Z.; Yu, Y. KMC Study on Byproduct Formation in the Process of Acetylene to Vinyl Acetate. *Industrial & Engineering Chemistry Research* **2020**, *59*, 13502-

13515, doi:10.1021/acs.iecr.0c02507.